

Evaluation of branch sampling, ocular assessments, and aerial surveys for estimating spruce budworm defoliation

Shawn Donovan and David A. MacLean 

Faculty of Forestry and Environmental Management, University of New Brunswick, P.O. Box 4400, Fredericton, NB E3B 5A3, Canada

Corresponding author: David MacLean (email: macleand@unb.ca)

Abstract

We compared three methods for estimating current-year spruce budworm (*Choristoneura fumiferana* (Clem.)) defoliation from 2014 to 2021 using a network of 99 permanent sample plots in central Gaspé Peninsula, Québec. Percent current-year defoliation was measured by assessing shoots from mid-crown branches, ocular ratings of all individual trees using binoculars, and provincial government aerial surveys. Ocular survey defoliation differed from branch sample defoliation in 5–6 out of 7 years, consistently underestimating defoliation, across the full range of defoliation severity observed. Nested mixed-effect models for fir–spruce combined, balsam fir, white spruce, and black spruce ocular survey defoliation bias resulted in marginal R^2 of 0.40, 0.47, 0.82, and 0.86, respectively. Current defoliation severity and its interaction with previous year defoliation and weather conditions significantly affected ocular survey bias. Correspondence of aerial survey estimates and mean plot defoliation occurred in only 43% of all plot-years and ranged from 14%–58% in individual years. Differences between aerial survey defoliation and plot values mainly resulted from assigning an adjacent class (e.g., light <30% assigned as moderate 31%–70% defoliation) or misplaced defoliation polygon boundaries, suggesting that assignment of aerial survey defoliation to plots or specific ground areas needs ground truth sampling.

Key words: defoliation, branch sampling, ocular estimation, aerial survey, spruce budworm

Introduction

Eastern spruce budworm (*Choristoneura fumiferana* (Clem.); SBW) is the most important natural disturbance agent in balsam fir (*Abies balsamea* (L.) Mill.)–spruce (*Picea* sp.) forests in eastern North America. SBW defoliation peaked at over 50 million hectares (ha) in the late 1970s (Blais 1983; Kettela 1983). SBW outbreaks, which typically last for 10+ years of annual defoliation, result in volume growth reductions of up to 90% (Ostaff and MacLean 1995) and tree mortality averaging 85% in mature balsam fir stands (MacLean 1980). During the 1970s–1990s SBW outbreak, defoliation caused 238 million m^3 of mortality in Québec (Coulombe Commission 2004), with economic losses estimated at \$12.5 billion (Lévesque et al. 2010). An SBW outbreak on 2.8 million ha of provincial Crown land in New Brunswick was projected to result in timber supply reductions of 29–43 million m^3 and economic losses of \$25–35 billion (Liu et al. 2019). Mitigation strategies for SBW outbreaks include (1) pre-outbreak silviculture or forest management to reduce balsam fir occurrence and increase less susceptible spruce, mixedwood, or hardwood stand types, (2) salvage harvesting severely defoliated stands, (3) aerial spraying of bioinsecticides (e.g., *Bacillus thuringiensis* var. *kurstaki* (Btk) or tebufenozide) for foliage protection to keep trees alive and growing, or (4) aerial spraying of insecticides under an early intervention strategy to identify and treat low but increasing SBW population “hot-spots”

before defoliation occurs (Johns et al. 2019; MacLean et al. 2019).

Forest managers rely on accurate estimates of annual defoliation at tree, stand, and landscape scales to inform forest protection operations, to monitor the changing extent and severity of SBW outbreaks, and to predict impacts on tree growth and mortality (e.g., MacLean et al. 2001). Defoliation can be assessed as the percentage of current-year needles removed, at the shoot, branch, tree, plot, or stand level, using one of four methods:

1. Branch sampling, also termed the shoot-count or Fettes method (Fettes 1950), is the most accurate and time-consuming method. One mid-crown branch per tree collected using pole pruners is the accepted sample for both SBW larval population and defoliation (Sanders 1980), with defoliation rated on a sample of current-year shoots, and a sufficient number of branches per plot assessed (MacLean and MacKinnon 1998). There were no significant differences in SBW defoliation among tree crown levels (Fettes 1950; MacLean and Lidstone 1982). MacLean and MacKinnon (1998) reported the number of shoots per branch and branches per plot required to estimate SBW defoliation with 90% or 95% probability that the 95% confidence interval is within $\pm 10\%$ defoliation; sample sizes varied as a function of tree species and defoliation

severity, with about 25 shoots/branch and a range of 7–24 branches per plot required. A shoot-count estimate of defoliation for a mid-crown branch had a relative error of $\pm 7\%$, compared to multiple samples per tree (MacLean and Lidstone 1982). The main advantage of the Fettes or shoot-count branch sampling of defoliation is having a branch in hand, so the observer can accurately identify current-year shoots and estimate the percentage of needles per shoot removed by SBW feeding.

2. Ocular surveys to rate defoliation of individual trees as a percentage of needles removed from current-year shoots are conducted by trained observers using binoculars. These use an identical measure of defoliation as branch sampling, but the observer is at some distance from the tree; he or she must first identify current-year shoots in the crown and estimate the mean percentage of needles removed on these current-year shoots throughout the crown. Ocular surveys are efficient and can have an error of $\pm 12\%$ with an experienced observer but can be biased towards overestimation at low defoliation levels (error 20%–30% defoliation), and previous-year severe defoliation can cause overestimation of current defoliation by 30%–40% (MacLean and Lidstone 1982).
3. Aerial surveys are commonly used to estimate current-year defoliation for large areas, during a 2–3 week period after SBW larval feeding ends, when the damaged or dead foliage turns reddish-brown. SBW is a wasteful eater and does not consume the entire needle; a distinct reddish-brown coloration of dry foliage appears, as a result of budworm severing and webbing together needles into a “feeding tunnel” in the process of feeding (MacLean and MacKinnon 1996). The degree of reddening of foliage is related to the percentage of needles removed. Observers in fixed- or rotary-wing aircraft systematically fly flight lines over defoliated forests and categorize areas into current-year defoliation categories, typically light (<30% of current-year foliage removed), moderate (30%–70%), and severe (>70%) (e.g., Carter and Lavigne 1993 for New Brunswick surveys; Candau et al. 2000 for Ontario). Aerial defoliation surveys are intended to delimit the extent and severity of current SBW feeding, are used for forest management planning (e.g., salvage harvesting and insecticide treatments), and provide a good measure of year-to-year fluctuations in SBW populations over large areas (Kettela 1983). However, in recent years, these regional aerial survey defoliation values have also been used to assign defoliation level at a plot or small area level, e.g., for evaluation of SBW defoliation effects on tree mortality (Houndode et al. 2021), catchment discharge (Sidhu et al. 2024), aquatic nutrient cycling (Woodman et al. 2021), landscape patterns of outbreak risk (McNie et al. 2023), habitat of woodland caribou and moose (Chagnon et al. 2022), and modulation of climate effects of tree growth (Boakye et al. 2022). Accuracy of aerial surveys has been found to vary from 32% (Donovan et al. 2021) to 82% (MacLean and MacKinnon 1996). Errors arise due to observer bias, incorrect georeferencing, poor weather conditions (high winds, heavy rains, or hail showers that remove the “red stage” foliage), or poor visibility (e.g., haze) during flights

(MacLean and MacKinnon 1996; Taylor and MacLean 2008).

4. Satellite remote sensing is recently being used for defoliation detection. Satellite remote sensing of defoliation is potentially less costly and subjective than aerial surveys (Hall et al. 2016; Rahimzadeh-Bajgiran et al. 2018). Sentinel-2-derived spectral vegetation indices, in particular red-edge indices, in Random Forest models were able to detect and classify SBW defoliation in three classes (nil, light, and moderate) with overall error of 17% (Bhattarai et al. 2020), although the reference data were derived from a roadside survey in which a spotter (passenger) observed the tree line from a slow-moving vehicle for signs of defoliation and rated it in four percentage classes. Recent Sentinel-2 satellites have higher spectral, spatial, and temporal resolutions and additional spectral bands in the red-edge regions, compared to Landsat, which make them suitable for timely detection of SBW defoliation (Bhattarai et al. 2020). Both New Brunswick and Québec provincial governments are using satellite imagery to detect SBW defoliation and supplement or replace aerial surveys (New Brunswick Department of Natural Resources and Energy Development (NBDNRED 2022, 2023); Québec Ministère des Forêts de la Faune et des Parcs (QMFFP 2022)). New Brunswick in 2021 and 2022 used Sentinel-2 imagery and change-detection tools developed in ArcGIS to map reduction in the photosynthetic capacity of fir or spruce, using the normalized difference red edge index (NBDNRED 2022). Québec used harmonized Landsat Sentinel data to calculate the normalized burn ratio vegetation index, which was translated into defoliation classes by aerial survey experts based on visual interpretation of nearby aerial surveys (QMFFP 2022).

In this study, we evaluated and compared ocular, branch sampling, and aerial survey methods of estimating current-year SBW defoliation, using an intensive defoliation dataset collected from 2014 to 2021 in 99 sample plots in the Gaspé Peninsula, Québec. More than 9500 branch samples and nearly 28 000 ocular tree defoliation assessments were conducted. Objectives were to (1) compare mean plot-level annual defoliation, by SBW host species, of ocular surveys versus branch sampling; (2) evaluate bias and the impact of SBW host species, defoliation severity, previous defoliation, weather conditions, and observer experience on accuracy of ocular defoliation estimates; and (3) compare 7 years of aerial survey defoliation relative to mean branch sample defoliation estimated at the plot level for the same areas.

Methods

Study area and sample plot design

The study area was in the central Gaspé Peninsula of Québec, a section of the Great Lakes–St. Lawrence Forest Region (Rowe 1972). It is characterized as a balsam fir–white birch (*Betula papyrifera* Marshall) mixed forest (Bélanger et al. 1992), with rolling topography, river valleys, and alluvial flats (Rowe 1972). SBW defoliation was first detected in the study

area by Québec government annual aerial surveys in 2012. Ninety-nine circular (400 m²; 22.6 m diameter) sample plots were established in 2014, usually with 3–5 plots an average of 100 m apart within stands. Plot locations were selected to represent balsam fir-dominated (>60%) stands and a range of current defoliation levels, with a target of 10 plots in each 10% current defoliation class (0%–10%, 11%–20%, etc.). From 2014 to 2021, salvage harvesting gradually reduced the total number of available plots to 56. Each plot tree ≥ 3 cm diameter at breast height (DBH; at 1.3 m) was measured for species, DBH, total and live crown heights, crown widths in the four cardinal directions, and location (distance and azimuth direction from plot center). Plot species compositions were dominated by SBW host species with 64% balsam fir, 19% black spruce, 9% white spruce, and 8% non-host species (percent basal area). Further description of the sample plot network is available in [Donovan et al. \(2018\)](#).

Annual assessment of current defoliation in sample plots

Defoliation was measured each year from 2014 to 2021, except for 2020 because of COVID travel restrictions, using both shoot-count and ocular survey methods. Sampling occurred soon after SBW feeding had ceased, in late July to early August. In the shoot-count method, pole pruners were used to collect one mid-crown branch from 15 randomly selected trees per host species per plot. One mid-crown branch is representative of defoliation on trees of all sizes ([Sanders 1980](#); [MacLean and Lidstone 1982](#)) and is a valid method for sampling SBW larval numbers ([Sanders 1980](#)) and defoliation ([MacLean and Lidstone 1982](#)). The largest variability in defoliation occurred between trees, not within trees; there were no significant differences in defoliation between tree quadrants (north, south, east, and west) or crown levels (top, middle, and bottom) ([Fettes 1950](#); [MacLean and Lidstone 1982](#)). Neither branch defoliation error nor ocular defoliation error are related to tree size (basal area). Sample sizes were based on [MacLean and MacKinnon \(1998\)](#), who sampled 172 000 individual shoots rated for SBW defoliation from nearly 7000 mid-crown branches and determined the number of shoots needed to estimate the mean defoliation per branch and number of branches (one mid-crown branch per tree) needed to estimate mean defoliation per plot, with a confidence interval of $\pm 10\%$ with 90% confidence. Sample sizes varied with the level of defoliation and ranged from 7 to 24 branches per plot and from 19 to 44 shoots per branch ([MacLean and MacKinnon 1998](#)), with the largest samples required at intermediate defoliation levels. In the current study, involving a large number of plots with varying defoliation levels assessed for 7 years, we used consistent sample sizes of one mid-crown branch from each of 15 trees per plot and defoliation assessed on each of 25 randomly selected current-year shoots per branch ([Fettes 1950](#)). In the shoot-count method, the observer estimates the percentage of needles that are missing or dead on each sampled shoot on a branch in hand. [MacLean and Morgan \(1981\)](#) evaluated visual estimates of individual shoots compared to counts of actual number of needles per shoot, assessed using the phyllotactic (spiral) arrangement of

needles on over 500 balsam fir shoots. Mean percent error per tree ranged from 1.2% to 6.0% and averaged 4.9%. For consistency, both ocular and branch sample methods used the same seven percentage defoliation classes: 0%, 1%–20%, 21%–40%, 41%–60%, 61%–80%, 81%–99%, and 100% ([Piene et al. 1981](#)).

The ocular defoliation estimation method also assessed percentage of needles missing or dead on current-year shoots on a tree, but by scanning the tree with binoculars, identifying current-year shoots throughout the crown, and assigning a mean percent defoliation class per tree. Observers were trained to identify current-year shoots using binoculars and in assigning the 20% defoliation classes, to consider the class midpoints in deciding “borderline” cases (e.g., if a single shoot or all shoots on a tree seemed to be about 40% defoliated, is it more like the 30% midpoint of the 21%–40% class or the 50% midpoint of the 40%–60% class?). It is feasible to estimate percent defoliation of the current shoots or cumulative defoliation of all shoots per tree and has been used in published studies since the 1970s. For ocular surveys, each SBW-host tree ≥ 10 cm DBH was assessed using binoculars by a trained observer viewing the entire tree crown for defoliation. In total over the 7 years, a total of 9541 branches were sampled and 27 962 individual tree ocular defoliation assessments were completed. The distribution of branches and trees sampled reflected the balsam fir-dominant plot composition: 70% of the branches and 77% of the trees sampled were balsam fir, 22% and 16% were black spruce, and 8% and 7% were white spruce.

We initially analyzed only the subset of trees from which branch samples were collected and compared ocular versus shoot-count defoliation estimates taken on the same trees (included as Supplementary Figs. S2 and S3), for all years combined ($n = 549$) and by year. We then calculated mean defoliation per plot weighted by tree basal area ([Hennigar et al. 2008](#)), which accounts for tree size such that larger trees with larger crowns and more foliage contribute more to mean plot defoliation. Mean annual ocular defoliation per species per plot was calculated by assigning class midpoints to each assessed tree, weighting defoliation by tree basal area to the total host-species basal area per plot, summing values, and dividing by number of trees. Mean annual branch defoliation per species per plot was calculated by averaging assessed current-year shoots per branch and branches per plot and weighting defoliation by the species basal area to total basal area per plot. We tested whether weighting by basal area significantly altered the correlation between shoot-count and ocular defoliation methods (Supplementary Fig. S1) and found identical correlation for the 7 years combined and annual correlation coefficient ranges of 0.65–0.89 (weighted; used in the text) versus 0.64–0.93 (unweighted; Supplementary Fig. S1).

Aerial surveys of SBW defoliation are possible because SBW larvae sever and web together needles in the process of feeding, which results in a distinct reddish-brown coloration with the degree of redness related to defoliation of current-year foliage ([Sanders 1980](#); [Kettela 1983](#); [Hardy et al. 1986](#); [MacLean and MacKinnon 1996](#)). Aerial surveys of SBW defoliation have been used by most provincial governments in Canada annually since the 1940s, generally using three defoliation classes

(light 11%–30%, moderate 31%–70%, and severe 71%–100%; areas with no noticeable defoliation assigned to a nil 0%–10%) class (e.g., Carter and Lavigne 1993). The specific Québec aerial survey is similar to that of other jurisdictions in assessing defoliation in three classes (light, moderate, and severe) and is carried out by airplane at an altitude of about 240 m at a speed of 200 km/h, with a distance of 4.5 km between the flight lines (Québec Ministère des Ressources Naturelles et des Forêts 2023). Defoliation is captured using a touch screen computer equipped with PC-Mapper software, making it possible to digitize in real time the damage observed from the air. To facilitate the work of the observer, a layer of polygons of susceptible stands merged with the contours of historical observations and a topographic map that reproduces the route of the plane are used and displayed in the background. The relationship between the reddish coloring of foliage to percent defoliation is well-established, has been used for decades, and is also apparent visually at the branch and tree level. Annual aerial defoliation survey data were provided by the Québec government (e.g., QMFFP 2021). Québec aerial surveys further describe the three defoliation classes as light—slight loss of foliage in the upper third of the crown; moderate—loss of foliage in the upper half of the crown of most trees; and severe—loss of foliage across the crown length of most trees (QMFFP 2021). To compare aerial survey defoliation with plot-level branch defoliation data, we assigned the three aerial defoliation classes as light <30%, moderate 30%–70%, and severe >70%; these are the percent defoliation class thresholds used in New Brunswick (MacLean and MacKinnon 1996), Ontario (Candau et al. 2000), and other jurisdictions (e.g., Waters et al. 1958; Dorais and Kettela 1982; Kettela 1983).

Comparing defoliation from ocular and aerial surveys with branch sampling

The measure of defoliation is the same in all three methods—namely percentage of current-year needles removed. SBW larvae strongly preferentially consume current-year foliage and will only feed on older age classes of foliage if all current-year foliage is gone. Defoliation is assessed directly in the shoot-count and ocular methods and via correlation with foliage reddening in the aerial surveys. The difference between the three methods is essentially scale or proximity of the observer to the defoliation and ease of accurate assessment of amount of defoliation. With the shoot-count method, the observer has a branch in hand, can easily identify current-year shoots, and examine each of 25 individual shoots to calculate a mean percent defoliation level for the branch. With the ocular method, the observer stands several meters from the tree and scans the crown with binoculars, identifying current-year shoots (most easily at the tips of branches), estimates in 20% classes how much current-year foliage has been removed, and assigns a class per tree. With aerial surveys, the observer is flying in an aircraft at 200 km/h speed, at an altitude of 240 m or higher, with flight lines 4.5 km apart, and is mainly observing the degree of redness of trees below. Both ocular and aerial survey accuracy are influenced by weather conditions and crown illumination con-

ditions; in fact, in some years, aerial surveys use fewer classes because of poor conditions (MacLean and MacKinnon 1996). In training field crews to conduct ocular defoliation assessments, good practice is to take branch samples from training trees, so the observer can identify current-year shoots and defoliation level close-up.

In this analysis, we assumed that detailed branch sampling with 15 mid-crown branches and assessing a total of 375 shoots per species per plot provided the most accurate assessment of current-year defoliation per plot. Branch sampling using the shoot-count method is the “gold standard” among the three methods, given that sufficient shoots per branch and branches per plot are sampled to provide the desired accuracy and confidence level to determine mean defoliation per plot (Fettes 1950; Sanders 1980; MacLean and Lidstone 1982; MacLean and MacKinnon 1998). We therefore compared mean ocular survey current-year defoliation (one binocular estimate per host tree per plot) with mean branch sample defoliation (15 mid-crown branches per plot), each year from 2014 to 2021 using Pearson’s correlations to assess the linear relationship and LOESS (locally estimated scatterplot smoothing) regression, a non-parametric technique that uses local weighted regression to fit a smooth curve through points in a scatter plot. LOESS was used because of indications of nonlinear relationships and was implemented using the “geom_smooth” function in the ggplot2 package, setting a confidence interval = 0.95 and span = 0.75 (Wickham 2016). Defoliation data from branch sampling and ocular surveys were first tested to determine whether normal data distributions existed and what parametric or non-parametric statistical comparison methods should be selected. The Shapiro–Wilk normality test analyzed the data distributions of defoliation per plot per year for each method using R statistical software (R Core Team 2023). Results indicated non-normal distributions for both datasets. Percent difference and bias of ocular and aerial surveys versus branch sampling were calculated for each plot. Non-parametric statistical pairwise tests between ocular survey and branch sampling percent defoliation per plot per year were completed using the Wilcoxon’s signed-rank and the two-sample Kolmogorov–Smirnov tests. The Wilcoxon’s signed-rank test evaluates a null hypothesis that the defoliation medians for the two methods are equal, while the Kolmogorov–Smirnov tests a null hypothesis that the two defoliation datasets have common shape distributions based on the cumulative distribution function. Results of the largest absolute difference between percent defoliation (test statistic D) and *p* value were reported for the Kolmogorov–Smirnov test.

To compare aerial survey defoliation with plot-level defoliation based on the Fettes method each year, the “spatial join tool” within ArcGIS Pro 3.1.3 (ESRI 2023) was used to identify the aerial survey defoliation polygon to which each plot belonged each year. Then for each year and plot, we assigned a defoliation class based on the value from the branch sampling and compared it with the class of the encompassing polygon. The fact that a plot had a different class than that of the encompassing aerial survey polygon is not evidence of a labeling error in the polygon, but we can assess, for each aerial survey category of polygons, over the 7 years sampled,

to what degree the Fettes-based defoliation of plots agreed with the class of their aerial survey polygon. Confusion matrices appropriate for summarizing classification data were generated for aerial survey data versus plot mean branch samples per year (Congalton 1991; Stehman and Foody 2019).

Mixed-effect modeling of variables influencing ocular survey defoliation bias

To examine covariates or factors affecting ocular survey defoliation bias, nested mixed-effect models were fit using R version 4.3.1. (R Core Team 2023) and the lme4 package (Bates et al. 2015). Nested mixed-effect models examined four tree species datasets based on response variables for plot-average ocular survey defoliation bias (e.g., percent current-year defoliation derived from the branch sample Fettes method minus ocular estimates) for all SBW host species, and single species datasets for balsam fir, white spruce, and black spruce. Fixed-effect explanatory variables included percent current branch defoliation severity, percent previous year ocular defoliation, percent previous cumulative ocular defoliation, and random-effect factors weather condition during ocular surveys (three levels: cloudy, sun/cloud, and sunny) and observer experience (two levels: no experience—trained during sampling and experienced—having at least 1 year of ocular survey experience). Similar variables were previously identified as influencing the precision and accuracy of ocular surveys of SBW defoliation in previous outbreaks (MacLean and Lidstone 1982). Nested mixed-effect models accounted for data dependence/sample plot resampling by defining a random-effect structure with sample plots nested within stands.

Identifying optimal nested mixed-effect models was achieved following general model selection guidelines and model assumption checks described by Zuur et al. (2009). Covariates were first rescaled by centering (e.g., subtracting their means from each observation), to reduce variable/interaction collinearity (Quinn and Keough 2002). Factors weather and observer experience were re-leveled setting sunny and experienced observers as model baseline reference levels, inferring ideal conditions for conducting ocular surveys. Model selection started with a beyond optimal nested mixed-effect models containing all variables and two-way interaction terms using maximum likelihood estimation of variance components. At each model iteration, a single term (starting with interaction terms) identified as the least significant based on Analysis of variance (Type III Satterthwaite's method) was dropped from successive models. Model performance was evaluated by metrics, including Akaike information criterion, Bayesian information criterion, conditional R^2 , marginal R^2 , and likelihood ratio tests. Additional consideration for identifying optimal models involved checking multicollinearity, which can reduce the accuracy of regression coefficient estimates making “true” effects harder to detect (Quinn and Keough 2002; Harrison et al. 2018). Variance inflation factors (VIFs) were calculated during each model iteration and variables with VIFs > 10 were considered problematic (Dormann et al. 2013), and models were further simplified until all VIFs < 10. Finally, optimal model summary performance was presented using restricted likelihood esti-

mation of variance components, which is less biased than maximum likelihood (Zuur et al. 2009).

Further interpretation of final models focused on the effect size of explanatory variable interactions and was completed by post-hoc comparisons of simple slopes. Simple slope analysis rather than comparing estimated marginal means is more appropriate when interaction terms include covariates. Interactions involving two covariates were explored by selecting representative grouping levels, namely the mean minus 1 standard deviation, the mean, and the mean plus one standard deviation as grouping levels, to aid in visualizing interaction effects. These resulted in low, moderate, and severe defoliation levels; for example, these values for current branch defoliation severity were 19%, 46%, and 72% defoliation all fir—spruce and 23%, 52%, and 80%, respectively, for balsam fir. Significance testing of slopes and visualization was completed using the emmeans package (Lenth 2023).

Results

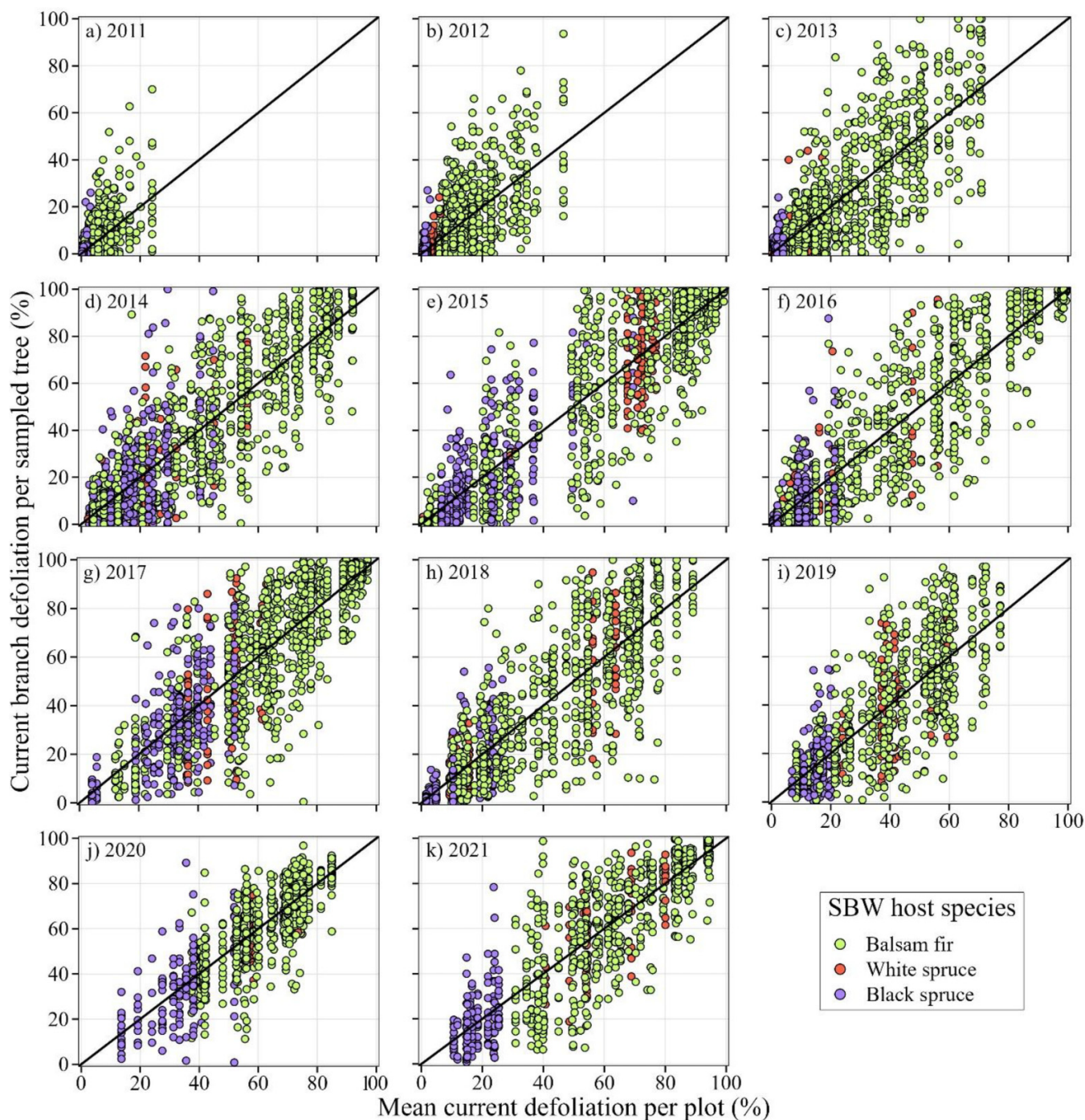
Variability in defoliation among branch samples, species, and years

The first defoliation (<30%) observed in the study plots occurred in 2011, based on sampling previous foliage age classes when the plots were established in 2014, and balsam fir trees were defoliated <50% in 2012 and <70% in 2013 (Fig. 1). The 2011–2013 data were excluded from subsequent accuracy analyses because they were available only for branch samples. There was considerable variability among branches sampled within a plot, species, and year, shown by the vertical “columns” of individual branch values for a given plot mean defoliation (Fig. 1). Black spruce defoliation was generally <60% for individual branches and <40% for plot means, while plot mean defoliation of white spruce was up to 80% and balsam fir was up to 100% (Fig. 1). It is noteworthy how widely defoliation varied among branches within a plot, especially at moderate plot mean levels, often ranging from <10% to >80% within a single plot and year (Fig. 1). Variability was lower for light and severe defoliation levels (Fig. 1).

Comparison of ocular survey and branch sampling defoliation

We initially compared ocular survey and branch sample defoliation using only the subset of trees sampled for both ($n = 1067$ – 1612 in 7 years; Supplementary Fig. S2). This showed wide variability within defoliation classes, Pearson's correlations ranging from 0.51 to 0.87 by year, an overall correlation of 0.74 for all years, and a consistent tendency to underestimate defoliation at high levels (Supplementary Fig. S2). Relationships for means per plot were similar, with Pearson's correlation coefficients of relationships between ocular and branch sample defoliation averaging 0.80 over 7 years and ranging from $r = 0.65$ – 0.89 , with 2016 and 2017 showing the highest and lowest correlations, respectively (Figs. 2a–2h). Mean defoliation per plot calculated without weighting by tree size had similar patterns (Supplementary Fig. S1). LOESS regressions showed that ocular survey estimates consistently underestimated branch sample defoliation, particu-

Fig. 1. Variability of current branch defoliation samples from 2011 to 2021 among host tree species plotted against mean branch defoliation per plot. Fifteen mid-crown branches were sampled in each plot each year, so vertical “columns” of data represent individual plot-years. Black lines represent the 1:1 relationship.

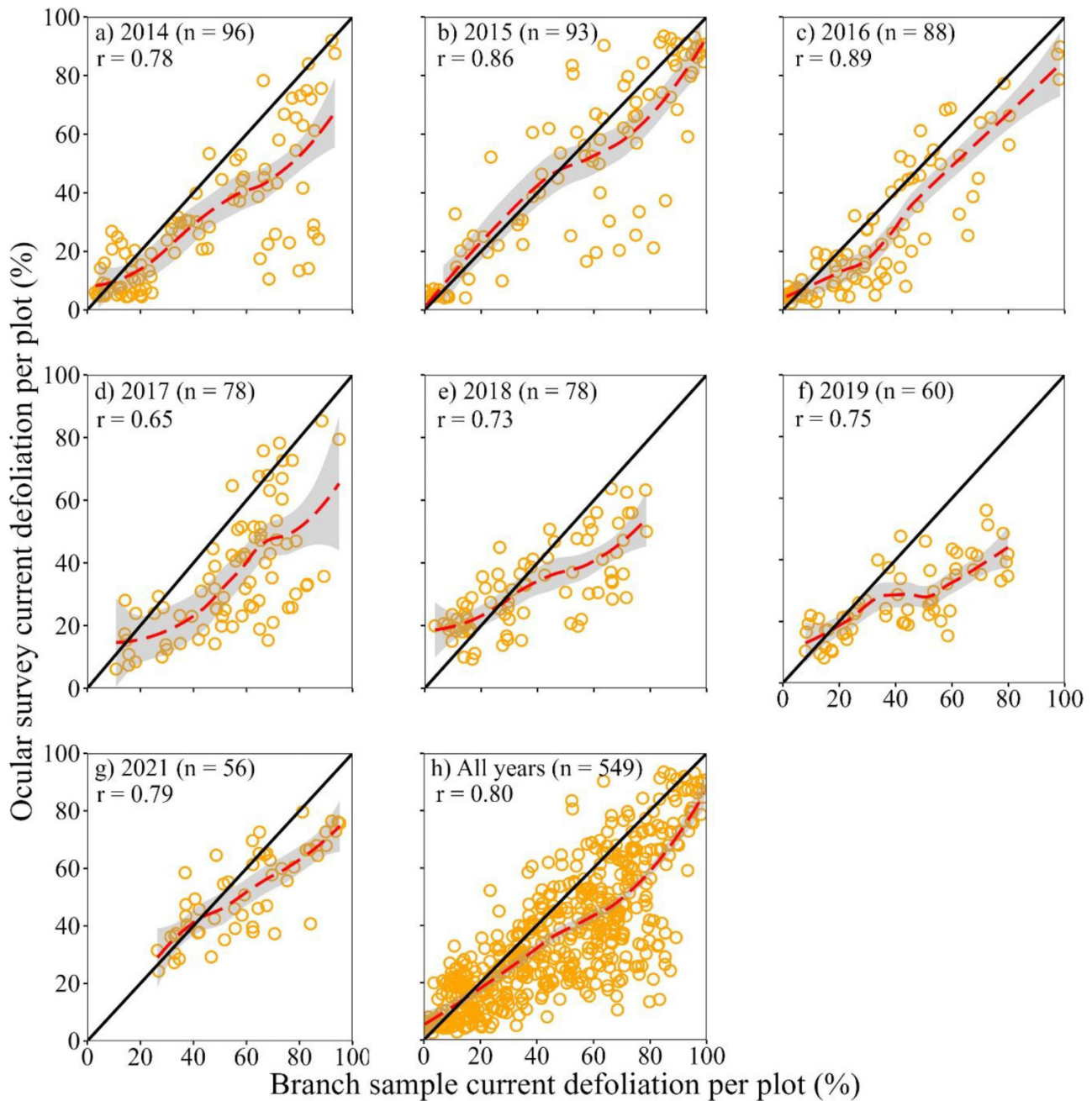


early at defoliation >50% (Fig. 2). The underestimates were greatest in 2017–2019 (Figs. 2d–2f) and least in 2015–2016 (Figs. 2b and 2c), and for all years combined, deviations declined at the highest defoliation levels (Fig. 2h).

Plotting ocular defoliation bias (i.e., plot mean branch sample minus ocular estimates) by year, for all fir–spruce combined and by species, showed that mean differences were consistently negative, with ocular surveys underestimating

defoliation (Fig. 3). For all fir–spruce combined, the ocular survey mean bias ranged from –5.2% in 2015 to –18.7% in 2017 (Fig. 3a). By species, ocular survey bias per year ranged from –15.4% to –30.2% for balsam fir (Fig. 3b), from –11.0% to –39.1% for white spruce (Fig. 3c), and from –3.2% to –20.3% for black spruce (Fig. 3d). About 20 plot-years had deviations >–60% for balsam fir (Fig. 3b), while only one case for black spruce and four cases for white spruce had ocular underesti-

Fig. 2. Comparison of mean ocular survey defoliation (one binocular estimate per host tree per plot) with mean branch sample defoliation (15 mid-crown branches per plot) from 2014 to 2021. Pearson's correlations (r) are reported measuring the linear relationship; LOESS regression lines (red dashed lines, with 95% confidence interval in grey) were fit each year, and the solid black line shows the reference 1:1 benchmark.



mates that large (Figs. 3c and 3d). Conducting a similar analysis using only the subset of branch sampled trees showed somewhat lower bias, especially for balsam fir and black spruce (Supplementary Fig. S3).

Wilcoxon's signed-rank pairwise testing of ocular survey versus branch sampling for all fir-spruce combined and by species showed that medians differed in all years and species except for black spruce in 2018 (Table 1). Two-sample Kolmogorov-Smirnov testing, comparing ocular surveys and branch sampling for all fir-spruce combined, rejected the

null hypothesis that the shape distributions were similar in 5 out of 7 years (all except 2015 and 2021) (Table 1). By species, Kolmogorov-Smirnov tests concluded that ocular surveys differed from branch sampling defoliation in all years for balsam fir and in 5 out of 7 years for black spruce and white spruce (Table 1). The D statistic reporting the largest absolute difference in pairwise comparisons for all fir-spruce combined ranged from 0.22 to 0.47 for tests rejecting the null hypothesis versus 0.11 and 0.23 in 2015 and 2021 when ocular and branch samples did not differ (Table 1).

Fig. 3. Box plots showing differences in mean plot-level ocular survey defoliation compared to mean defoliation of 15 branches sampled per plot, by spruce budworm host species and year. Hollow black circles represent individual sample plot data and the red x's are the annual means.

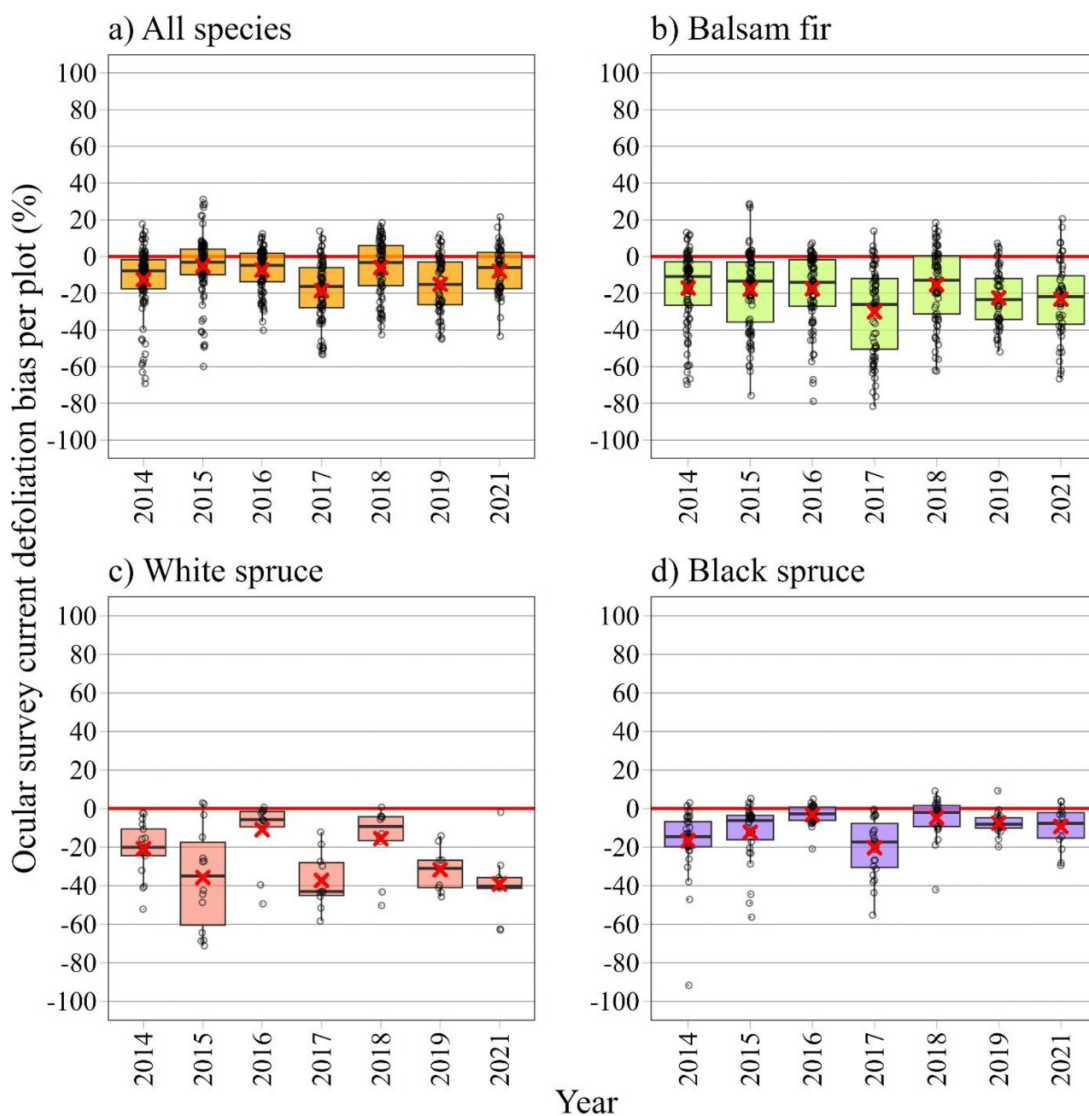


Table 1. Non-parametric pairwise Wilcoxon's signed-rank and two-sample Kolmogorov-Smirnov test results comparing ocular survey and branch sampling of plot-level annual defoliation from 2014 to 2021.

Year	Kolmogorov-Smirnov test ^a				Wilcoxon's signed-rank test ^c							
	p value				D statistic ^b				p value			
	All species	Balsam fir	Black spruce	White spruce	All species	Balsam fir	Black spruce	White spruce	All species	Balsam fir	Black spruce	White spruce
2014	0.01	<0.01	<0.01	<0.01	0.25	0.32	0.82	0.77	<0.01	<0.01	<0.01	<0.01
2015	0.66	<0.01	0.02	0.01	0.11	0.29	0.40	0.64	0.003	<0.01	<0.01	<0.01
2016	0.02	<0.01	0.04	0.26	0.23	0.34	0.40	0.42	<0.01	<0.01	0.02	<0.01
2017	<0.01	<0.01	<0.01	<0.01	0.47	0.58	0.70	0.90	<0.01	<0.01	<0.01	<0.01
2018	0.02	<0.01	0.24	0.05	0.24	0.38	0.30	0.60	0.01	<0.01	0.06	<0.01
2019	<0.01	<0.01	<0.01	<0.01	0.42	0.52	0.68	0.89	<0.01	<0.01	<0.01	<0.01
2021	0.10	<0.01	0.39	<0.01	0.23	0.45	0.33	0.89	<0.01	<0.01	<0.01	<0.01
All years	<0.01	<0.01	<0.01	<0.01	0.22	0.35	0.43	0.57	<0.01	<0.01	<0.01	<0.01

Note: Non-significant cases (i.e., where both methods led to similar results) are **bolded**.

^aThe Kolmogorov-Smirnov tests a null hypothesis that the defoliation results from both methods have a common shape distribution based on the cumulative distribution function.

^bThe D statistic reports the largest absolute difference between pairwise comparisons.

^cThe Wilcoxon's signed-rank tests a null hypothesis indicating that the defoliation medians for the two methods are similar.

Table 2. Nested mixed-effect model summaries for final models examining ocular survey defoliation bias (%) combining all SBW host species (ALL), balsam fir (BF), white spruce (WS), and black spruce (BS) estimates.

Final model	Sample plot observations	No. var. ^a	Final model's explanatory variables ^b	Model goodness-of-fit performance ^c	
				Cond. R ²	Marg. R ²
ALL7	549	9	CBDS + PYCD + PCuD + W + OE + CBDS*PYCD + CBDS*W + PYCD*OE + CBDS*PCuD	0.55	0.40
BF5	527	11	CBDS + PYCD + PCuD + W + OE + CBDS*PYCD + CBDS*W + PYCD*OE + CBDS*PCuD + PYCD*PCuD + W*OE	0.77	0.48
BF10	527	3	CBDS + PYCD + CBDS*PYCD	0.71	0.47
WS10	81	3	CBDS + W + CBDS*W	0.92	0.82
WS11	81	2	CBDS + W	0.91	0.80
BS11	167	2	CBDS + PYCD	0.92	0.86

Note: Supplementary Tables S1–S5 summarize model testing and selection and final explanatory variable significance, variance inflation factors, and effect sizes.

^aNumber of explanatory variables (plus interaction terms) included in final models.

^bExplanatory variable abbreviations: previous year current ocular defoliation (PYCD); previous cumulative ocular defoliation (PCuD); current branch defoliation severity (CBDS); weather condition (W); and observer experience (OE).

^cConditional R² explains model variance for both fixed- and random effects, whereas the marginal R² explains the variance only for fixed effects. Model results are presented using the less biased method of estimating the variance components known as restricted maximum likelihood.

Variables and factors influencing ocular survey defoliation bias

Details of selection of the best nested mixed-effect model analyses of ocular defoliation bias are presented in Supplementary Tables S1–S4. The final models varied in complexity among all fir–spruce species (ALL), balsam fir (BF), white spruce (WS), and black spruce (BS) (Table 2). The BF and ALL models were complex including 11 and 9 variables and interactions significantly affecting ocular bias, whereas the WS and BS models had only 3 and 2 variables, respectively (Table 2). Simplified models for BF and WS with only 3 and 2 variables were almost as good as the best models (Table 2). Ocular defoliation bias was significantly affected by current branch defoliation severity in all grouped fir–spruce and individual tree species models, and previous year current defoliation, weather, and their interactions were also significant (Table 2). Only the most complex models for ALL and BF included observer experience and previous cumulative defoliation (Table 2). Ocular bias model goodness-of-fit metrics conditional R² and marginal R² were highest for BS11 (0.92, 0.86) and WS10 (0.92, 0.82) models and lower for ALL7 (0.55, 0.40) and BF10 (0.71, 0.47) models (Table 2).

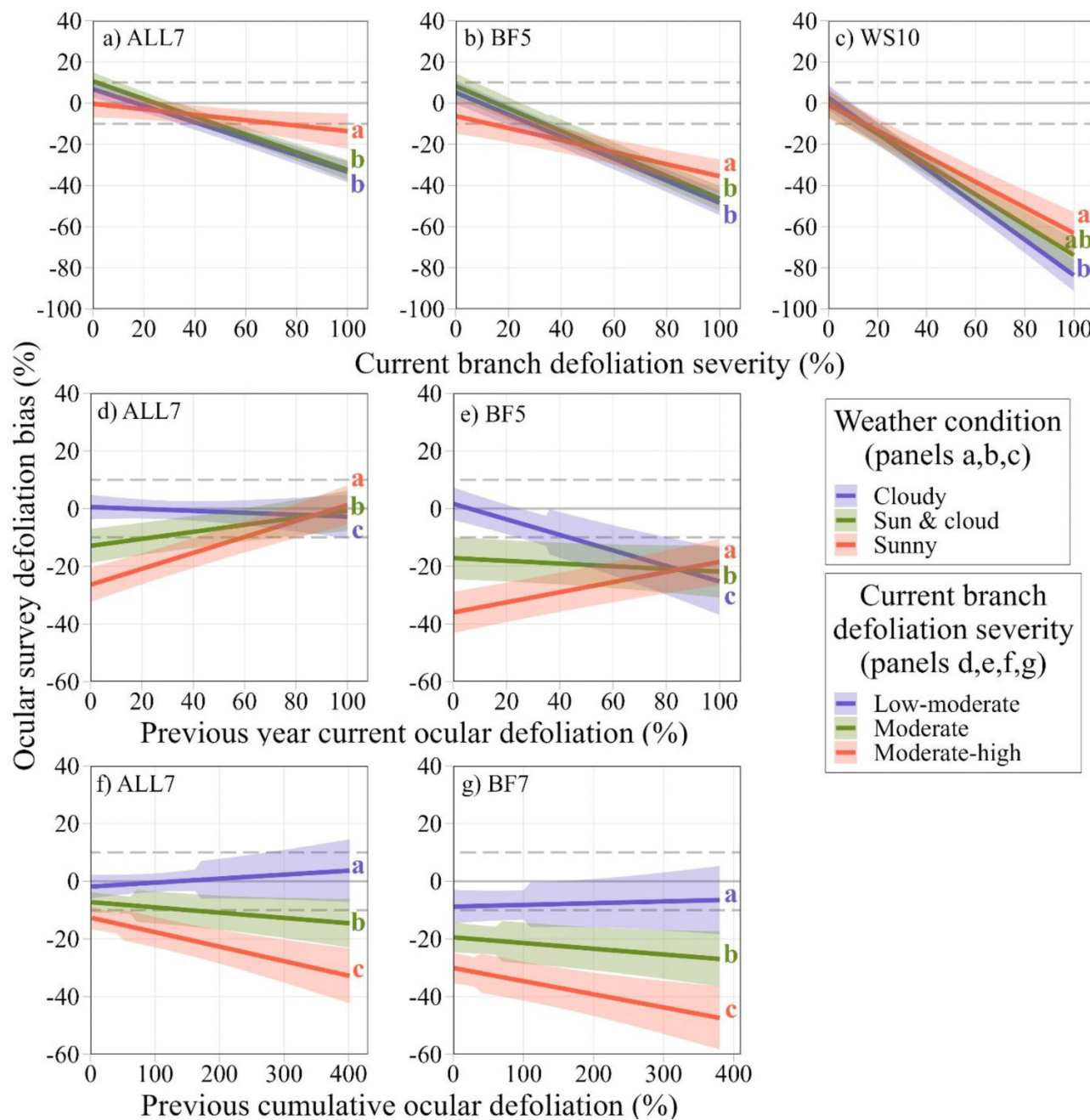
We have displayed ocular bias model interaction term effect sizes in Figs. 4 and 5 based on estimated simple slope differences. Ocular defoliation underestimation bias increased with current branch defoliation severity under all weather (cloudiness) conditions (Figs. 4a–4c). However, underestimation bias was significantly less under sunny weather conditions than under either sun and cloud or cloudy conditions when current branch defoliation severity was ~20%–50% (Figs. 4a–4c). Ocular bias for the ALL species model was low under low current defoliation and all previous year defoliation levels, but under moderate and severe current defoliation, underestimation decreased with increasing previous year defoliation (Fig. 4d). Ocular defoliation underestimation generally was greater for severe than moderate or light current defoliation (Figs. 4d–4g) and increased with previous cumulative defoliation (Figs. 4f–4g).

Ocular defoliation underestimation was low for experienced observers under all previous year defoliation levels but decreased as previous year current defoliation increased for inexperienced observers (Figs. 5a and 5b). Bias was significantly lower for experienced observers under both sun and cloud and sunny conditions (Fig. 5c). The ocular bias model for BS contained only main effects of current branch defoliation severity, which had a large effect size (Supplementary Table S5) indicating a strong negative relationship with ocular survey bias with a correlation of $r = -0.91$ (Fig. 5d), and previous year defoliation, which had a positive trend but with a smaller effect size (Supplementary Table S5) and smaller correlation of $r = 0.23$ (Fig. 5e). Ocular defoliation bias for BF had an interaction between previous cumulative defoliation grouped by previous year defoliation, which indicated a constant negative bias of ~20% with severe previous year current defoliation across the full range of previous cumulative defoliation (Fig. 5f), but under low-moderate previous year defoliation, ocular survey bias became increasingly negative with increasing previous cumulative defoliation (Fig. 5f). Additional variable significance and effect size results are presented in Supplementary Table S5. Large effect sizes (~0.14; Cohen 1988) occurred for current branch defoliation severity (0.20 for ALL fir–spruce, 0.41–0.51 for BF, 0.90 for WS, and 0.89 for BS), for weather (WS 0.14 and interaction with current branch defoliation 0.14), and previous year current defoliation (BS 0.32).

Comparison of aerial survey and branch sampling defoliation

When the plot-level defoliation from branch sampling was compared with the defoliation class of the encompassing aerial survey polygon, there were discrepancies in more than half of the cases (Fig. 6). Percentage of plots with branch defoliation in the same class as the aerial survey value averaged 58%, 47%, and 38% for plots with light, moderate, and severe defoliation, respectively (Fig. 6). These values varied greatly from year to year, with the cases where plot branch sample defoliation and aerial survey defoliation classes were the

Fig. 4. Interaction plots of estimated simple slopes of ocular survey defoliation bias from final models for all species (ALL7), balsam fir (BF5), and white spruce (WS11). Ocular survey defoliation bias was significantly affected by (a–c) current branch defoliation severity grouped by weather conditions, (d and e) previous year current defoliation grouped by current branch defoliation severity, and (f and g) previous cumulative defoliation severity. Shaded areas represent confidence intervals.



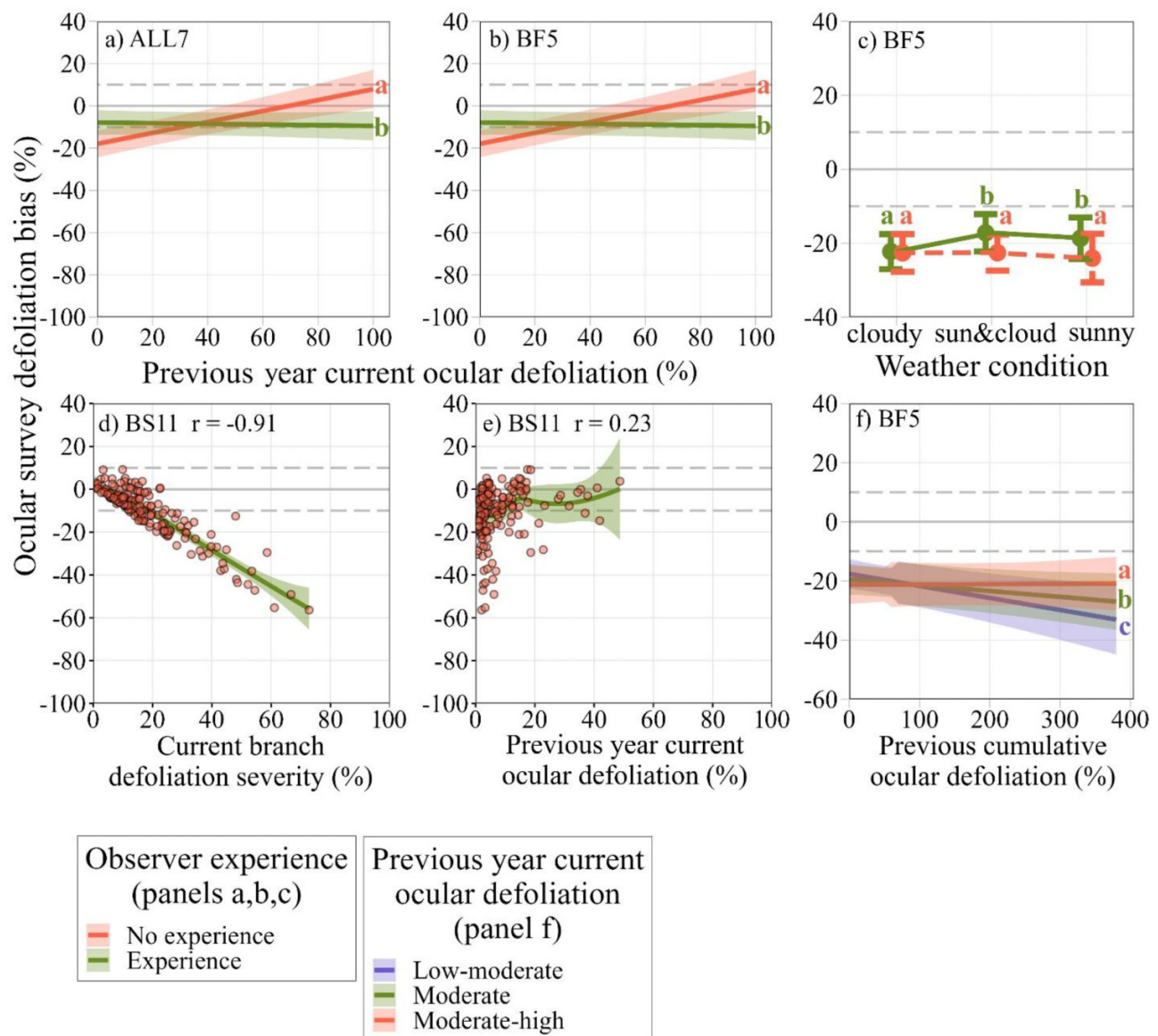
same ranging from 4% to 94%, 33% to 59%, and 9% to 100% for light, moderate, and severe defoliation classes, respectively (Fig. 6).

A confusion matrix comparing aerial survey defoliation versus mean branch sample defoliation across plots and years showed that the severe defoliation class had the most discrepancies, with only 28% of cases agreeing, followed by the moderate class at 45%, and the light class at 51% (Table 3). Differences between aerial survey and plot branch sample values were mainly for the adjacent defoliation class: moderate for

light and vice versa, and moderate for severe (Table 3). Overall for all 7 years combined, 43% of plots had the same branch sample and aerial survey defoliation classes (Table 4), and by year, percentage of plots with the same defoliation class rating were 38%, 56%, 47%, 46%, 37%, 58%, and 14% for 2014–2021, respectively (Table 4). The largest difference, in 2021, resulted from aerial surveys classifying all plots as light defoliation.

Several examples of plot-level branch sample defoliation overlaid on aerial survey defoliation polygons demonstrate

Fig. 5. Interaction plots of estimated simple slopes of ocular survey defoliation bias from final models for all species (ALL7), balsam fir (BF5), and black spruce (BS11). Ocular survey defoliation bias was significantly affected by (a and b) previous year current ocular defoliation severity grouped by observer experience, (c) weather condition grouped by observer experience, (d and e) main effects of current branch defoliation severity and previous year current ocular defoliation for black spruce, and (f) previous cumulative defoliation grouped by previous year current defoliation. Shaded areas represent confidence intervals.



common differences (Fig. 7). One was mislocated aerial defoliation polygon boundaries (i.e., close but not quite correct). This was evident for stand 26 (Fig. 7a), where the aerial survey light defoliation boundary was south of the plot locations; in stand 10 (Fig. 7b), with the moderate defoliation boundary just to the left of four moderate plot locations; and in stand 6 (Fig. 7c), where the five plots all with moderate defoliation were within a severe defoliation polygon but slightly to the right there was a moderate polygon. Figures 7d–7f show three examples with the same defoliation class from aerial surveys and plot branch sampling. In contrast, Figs. 7g–7i show three examples of substantial differences of severe aerial survey values when branch sample defoliation was light (Figs. 7g and 7h) and vice-versa (Fig. 7i).

Discussion

Aerial surveys of SBW defoliation have been used routinely for over 80 years in Canada and the United States (Hardy et al. 1986), and branch sampling and ocular methods have been used in monitoring and research studies for many decades. Accurate defoliation at the tree and plot level is the “lynch-pin” required to quantify and model effects of defoliation on tree growth and mortality (e.g., Erdle and MacLean 1999). We accumulated a large, unique dataset from seven sample years, with over 9500 branch samples and nearly 28 000 ocular tree defoliation assessments, which was well-suited to compare the three methods.

Fig. 6. Ordinal distribution of branch-based percent defoliation of plots (along the x axis, in subsets of light <30% in green, moderate 31%–70% yellow, and severe >70% red) compared to aerial survey defoliation polygons in the same three classes, from 2014 to 2021. In an ideal (correct) scenario where defoliation is uniform throughout the polygon and the polygon has the correct label, all dots should be in the right panel for the severe class, in the middle panel for the moderate, and the left for the light. The table values represent the percentage of plots per defoliation class per year in each panel with correct values shown in bold.

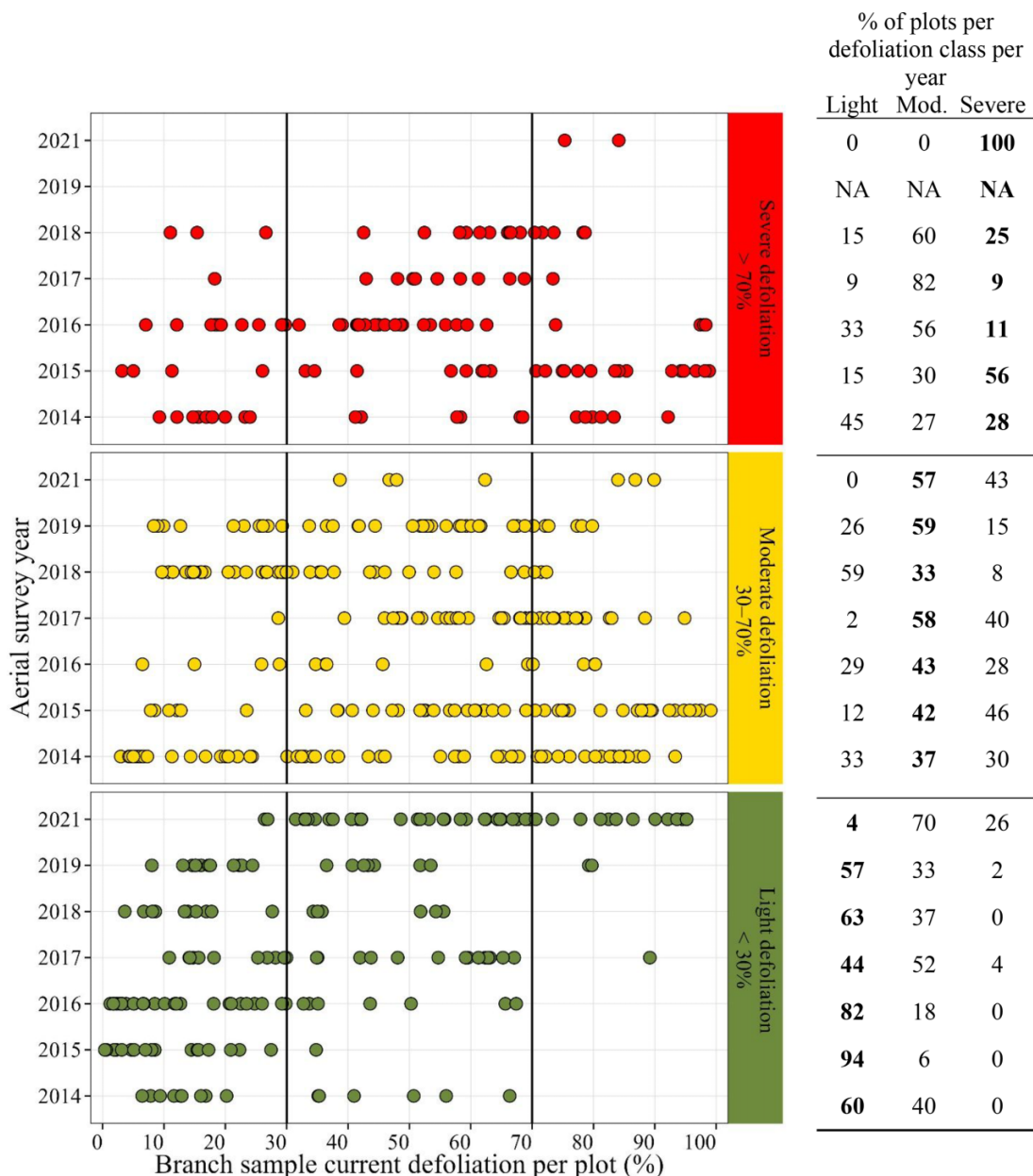


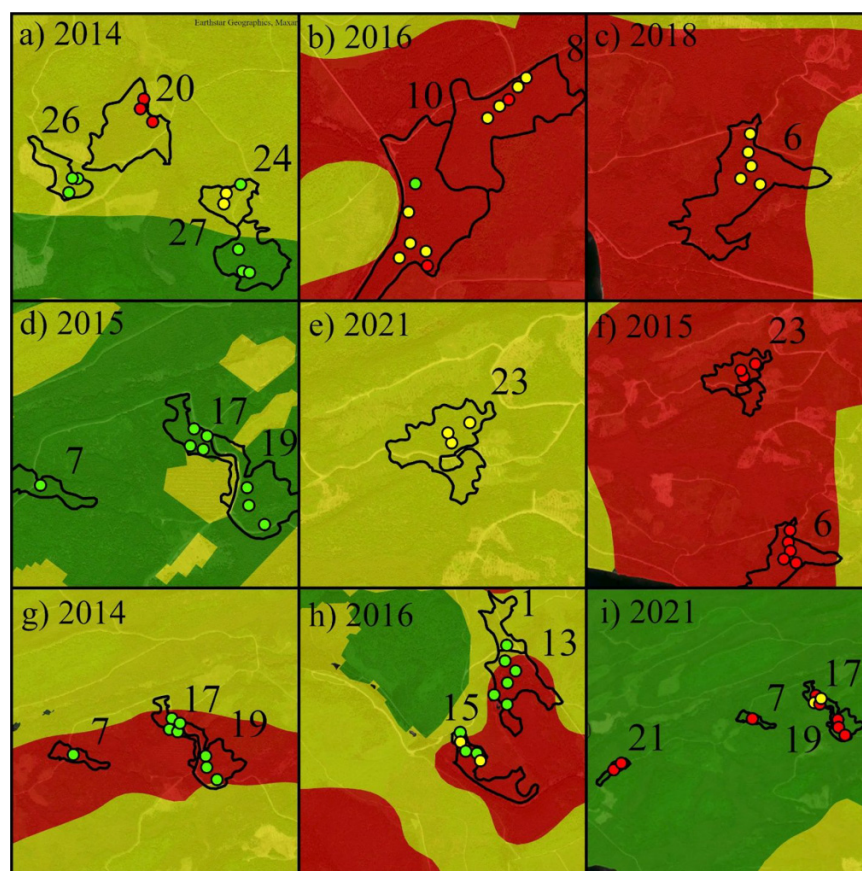
Table 3. Confusion matrix comparing annual defoliation class from aerial surveys with plot-level branch defoliation, combining 2014–2021 sample years.

		Branch sample defoliation class			Total	% of cases with aerial and branch defoliation in the same class
		Light (<30%)	Moderate (30%–70%)	Severe (≥70%)		
Aerial survey defoliation class	Light	93	74	15	182	51.1
	Moderate	63	110	71	244	45.1
	Severe	30	55	33	118	28.0
	Total	186	239	119	544	43.4

Note: Values are number of plots. Aerial and branch sample defoliation in the same class are in **bold font**.

Table 4. Percent agreement by class and year (2014–2021) between branch-based plot defoliation and defoliation class of the corresponding aerial survey polygon for the set of ground plots.

Year	No. plots	% of cases with aerial and branch defoliation in the same class, by defoliation class			Overall
		Light ($\leq 30\%$)	Moderate (30–70%)	Severe ($\geq 70\%$)	
2014	94	60	37	27	38
2015	93	94	42	56	56
2016	88	82	43	11	47
2017	78	44	58	9	46
2018	75	63	33	25	37
2019	60	57	59	NA	58
2021	56	4	57	100	14
All years	544	51	45	28	43

Fig. 7. Examples comparing branch plot defoliation (shown as colored circles: light in green, moderate in yellow, and severe in red) versus aerial survey defoliation polygons (the background colors, using the same three classes). Black lines and numerals represent sample stand boundaries and stand numbers. The scale differs among panels.

Our results showing an underestimation bias in ocular defoliation compared to branch sampling were also found using a much smaller sample size by MacLean and Lidstone (1982). Ocular methods tended to overestimate at light levels of defoliation (MacLean and Lidstone 1982), and our analysis suggested a similar pattern in the 2014, 2018, and 2019 defoliation measurements. The tests of ocular defoliation reported by MacLean and Lidstone (1982) showed that an experienced observer was generally 5%–10% closer to the true defoliation than a less experienced observer. In con-

trast, we used seasonal crews, sometimes with returnees, over the 7 years of sampling. Extensive observer training, ideal sunny clear skies, and timing defoliation assessments near the peak detection period should promote more consistency for the ocular survey method. The underestimation bias was lowest for black spruce (which consistently had the lowest defoliation level, also shown by Hennigar et al. (2008)) and greatest for white spruce, which produces the largest amount of foliage that can obscure partial defoliation.

Our detailed nested mixed-effect model assessment of factors influencing ocular defoliation accuracy is unique. Some of the results corroborate earlier work, that experienced observers had lower ocular defoliation underestimation. As expected, well-lit tree crowns under sunny conditions reduced ocular defoliation underestimation. But by far, the strongest effect for all fir–spruce combined and by species was that current branch defoliation level most strongly affected ocular defoliation bias, in interaction with previous year current and cumulative defoliation (tree-level and ocular estimates). In general, the more severe the actual defoliation (i.e., current branch defoliation) was, the greater the underestimation bias. This was magnified further with higher previous year cumulative defoliation. These tendencies should be taught during training of crews to assess current and cumulative defoliation. We typically use “blind” assessments of trees with known (branch sampled) defoliation levels in training crews.

When the defoliation class of the aerial survey polygon encompassing a given plot was compared to that derived from branch sampling, only 43% of plots had the same branch sample and aerial defoliation class. This demonstrates that caution should be used in ascribing aerial survey defoliation values to specific plots, stands, or other specific locations. Aerial surveys of spruce budworm defoliation are available every year during outbreaks in most jurisdictions and have often been used to assign defoliation to individual ground locations or plots. A common practice is to assume that all locations within an aerial survey polygon have the same defoliation level as the class assigned to the polygon, and to use it to assign a defoliation value. Alas, examples of such extrapolation of aerial SBW defoliation data in recent published studies include [Houndode et al. \(2021\)](#), [Woodman et al. \(2021\)](#), [Boakye et al. \(2022\)](#), [Chagnon et al. \(2022\)](#), [McNie et al. \(2023\)](#), and [Sidhu et al. \(2024\)](#). Yet there can be considerable variability and although the majority of stands within an aerial survey polygon are expected to have the severity level indicated in the polygon label, there can be areas within the polygon with differing levels of severity. This is not an error per se but a requirement of the aerial survey generalization. This is not to say that aerial surveys are inaccurate. [MacLean and MacKinnon \(1996\)](#) found 82% classification accuracy of aerial SBW surveys in New Brunswick between 1984 and 1993. [Coleman et al. \(2018\)](#) evaluated accuracy of aerial detection surveys for mapping insect and disease disturbances in the United States and concluded that overall accuracy of aerial detection observations was >70%. However, assuming that aerial survey defoliation accurately represents the level in specific locations within a polygon needs caution and ideally ground verification.

The use of aerial surveys in defoliation monitoring is in a time of transition, with several jurisdictions already moving to partially or fully switch to satellite imagery ([NBDNRED 2022, 2023](#); [QMFFP 2022](#)). [Donovan et al. \(2018\)](#) explored the use of hemispherical images of the canopy taken from the ground as a potential alternative to branch sampling and ocular surveys and found that image canopy gap fraction change from May to October combined with data on occurrence of aerial spraying of bioinsecticides and balsam fir per-

cent basal area could predict percent annual defoliation with root mean square errors ranging from 14% to 22%. [Kálin et al. \(2019\)](#) demonstrated that tree defoliation estimation from ground-level RGB images with a convolutional neural network worked well and achieved performance close to human experts (only 0.9% worse). Drone-based point clouds from lidar or photogrammetry also have good potential for assessing defoliation at the plot or stand level (e.g., [Cardil et al. 2017](#)) but may be limited for large regional assessments. Satellite remote sensing is of interest because of new sensor technology and improved image availability. [Rahimzadeh-Bajgiran et al. \(2018\)](#) assessed the use of Landsat-5 Thematic Mapper data to detect current defoliation and found classification accuracies of 77%, 60%, 52%, and 77% for nil, light, moderate, and severe defoliation classes, respectively. Sentinel-2 imagery classified annual defoliation using roadside defoliation observations as validation, and the Random Forest classification algorithm reported overall accuracy of 71% across nil, light, and moderate defoliation classes ([Bhattarai et al. 2020](#)). Finally, vegetation index changes calculated from satellite hyperspectral imagery for classifying three annual defoliation classes resulted in overall accuracies of 59% and 64% for Support Vector Machine and Random Forest classifiers, respectively ([Donovan et al. 2021](#)).

Branch sampling using the Fettes shoot-count method is the “gold standard” to quantify mean defoliation per plot, given that sufficient shoots per branch and branches per plot ([MacLean and MacKinnon 1998](#)) are sampled to provide the desired accuracy and confidence level. Ocular defoliation estimates are the primary method of obtaining individual-tree defoliation levels throughout plots, but accurate estimation requires crew training and is influenced by defoliation severity (current year, previous year, and cumulative), sky viewing conditions (sunny versus cloudy), and observer experience. When we compared the plot-level defoliation from branch sampling with the defoliation class of the encompassing aerial survey polygon, there were discrepancies in more than half of the cases. One cannot assume that an aerial survey defoliation polygon value is representative of all specific ground location within that polygon. The use of satellite remote sensing appears to be a valid option to use in conjunction with, or to replace, annual aerial surveys for improving SBW defoliation detection and outbreak monitoring but should be evaluated for accuracy compared with plot-level branch sampling data.

Acknowledgements

We thank the many summer field assistants who helped sample the thousands of branches and trees for defoliation in this study, from 2014 to 2021. This research was overseen by the Healthy Forest Partnership, a consortium of researchers, landowners, forestry companies, governments, and forest protection experts in Atlantic Canada. We thank the Québec Ministère des Forêts de la Faune et des Parcs for permission to use their SBW aerial survey defoliation data. We are grateful to Myriam Barbeau and René Malenfant for advice on mixed-effect modeling, and to the journal reviewers whose detailed comments improved the paper.

Article information

History dates

Received: 12 October 2023

Accepted: 13 February 2024

Accepted manuscript online: 16 February 2024

Version of record online: 15 May 2024

Copyright

© 2024 The Author(s). This work is licensed under a [Creative Commons Attribution 4.0 International License](https://creativecommons.org/licenses/by/4.0/) (CC BY 4.0), which permits unrestricted use, distribution, and reproduction in any medium, provided the original author(s) and source are credited.

Data availability

Data generated or analyzed during this study are available from the corresponding author upon reasonable request.

Author information

Author ORCIDs

David A. MacLean <https://orcid.org/0000-0002-0314-4435>

Author contributions

Conceptualization: DAM

Data curation: SD

Formal analysis: SD

Funding acquisition: DAM

Investigation: SD

Methodology: SD, DAM

Project administration: DAM

Resources: DAM

Software: SD

Supervision: DAM

Visualization: SD

Writing – original draft: SD

Writing – review & editing: SD, DAM

Competing interests

The authors declare that they have no known competing financial interests or personal relationships that could have appeared to influence the work reported in this paper.

Funding information

This research was funded by the Atlantic Canada Opportunities Agency, Natural Resources Canada, Government of New Brunswick, and forest industry in New Brunswick under the Early Intervention Strategy Against Spruce Budworm program.

Supplementary material

Supplementary data are available with the article at <https://doi.org/10.1139/cjfr-2023-0240>.

References

- Bates, D., Maechler, M., Bolker, B., and Walker, S. 2015. Fitting linear mixed-effects models using lme4. *J. Stat. Softw.* **67**(1): 1–48. doi:[10.18637/jss.v067.i01](https://doi.org/10.18637/jss.v067.i01).
- Bélanger, L., Bergeron, Y., and Camiré, C. 1992. Ecological land survey in Québec. *For. Chron.* **68**: 42–52. doi:[10.5558/tfc68042-1](https://doi.org/10.5558/tfc68042-1).
- Bhattarai, R., Rahimzadeh-Bajgiran, P., Weiskittel, A., and MacLean, D.A. 2020. Sentinel-2 based prediction of spruce budworm defoliation using red-edge spectral vegetation indices. *Remote Sens. Lett.* **11**(8): 777–786. doi:[10.1080/2150704X.2020.1767824](https://doi.org/10.1080/2150704X.2020.1767824).
- Blais, J.R. 1983. Trends in the frequency, extent, and severity of spruce budworm outbreaks in eastern Canada. *Can. J. For. Res.* **13**: 539–547. doi:[10.1139/x83-079](https://doi.org/10.1139/x83-079).
- Boakye, E.A., Houle, D., Bergeron, Y., Girardin, M.P., and Drobyshev, I. 2022. Insect defoliation modulates influence of climate on the growth of tree species in the boreal mixed forests of eastern Canada. *Ecol. Evol.* **12**: e8656. doi:[10.1002/ece3.8656](https://doi.org/10.1002/ece3.8656).
- Candau, J.-N., Fleming, R.A., Hopkins, A., and Perera, A.H. 2000. Characterizing spruce budworm caused disturbance regimes in Ontario. *In Disturbance in boreal forest ecosystems: human impacts and natural processes.* USDA For. Serv. Gen. Tech. Rep. NC-209. pp. 132–139.
- Cardil, A., Vepakomma, U., and Brotons, L. 2017. Assessing pine processionary moth defoliation using unmanned aerial systems. *Forests*, **8**: 402. doi:[10.3390/f8100402](https://doi.org/10.3390/f8100402).
- Carter, N.E., and Lavigne, D.R. 1993. Protection spraying against spruce budworm in New Brunswick 1992. N.B. Department of Natural Resources and Energy, Fredericton, NB.
- Chagnon, C., Bouchard, M., and Potheir, D. 2022. Impacts of spruce budworm defoliation on the habitat of woodland caribou, moose, and their main predators. *Ecol. Evol.* **12**: e8695. doi:[10.1002/ece3.8695](https://doi.org/10.1002/ece3.8695).
- Cohen, J. 1988. *Statistical power analysis for the behavioral sciences.* 2nd ed. L. Erlbaum Associates.
- Coleman, T.W., Graves, A.D., Heath, Z., Flowers, R.W., Hanavan, R.P., Cluck, D.R., and Ryerson, D. 2018. Accuracy of aerial detection surveys for mapping insect and disease disturbances in the United States. *For. Ecol. Manage.* **430**: 321–336. doi:[10.1016/j.foreco.2018.08.020](https://doi.org/10.1016/j.foreco.2018.08.020).
- Congalton, R.G. 1991. A review of assessing the accuracy of classifications of remotely sensed data. *Remote Sens. Environ.* **37**: 35–46. doi:[10.1016/0034-4257\(91\)90048-B](https://doi.org/10.1016/0034-4257(91)90048-B).
- Coulombe Commission (Commission d'étude sur la gestion de la forêt publique québécoise). 2004. Chapitre 4: protection, conservation et gestion multiressource: des axes de changement. *In Commission d'étude sur la forêt publique québécoise, Rapport final; Ministère des Forêts, de la Faune et des Parcs, Québec, QC.* pp. 47–92.
- Donovan, S.D., MacLean, D.A., Kershaw, J.A., and Lavigne, M.B. 2018. Quantification of forest canopy changes caused by spruce budworm defoliation using digital hemispherical imagery. *Agric. For. Meteorol.* **262**: 89–99. doi:[10.1016/j.agrformet.2018.07.006](https://doi.org/10.1016/j.agrformet.2018.07.006).
- Donovan, S.D., MacLean, D.A., Zhang, Y., Lavigne, M.B., and Kershaw, J.A. 2021. Evaluating annual spruce budworm defoliation using change detection of vegetation indices calculated from satellite hyperspectral imagery. *Remote Sens. Environ.* **253**: 112204. doi:[10.1016/j.rse.2020.112204](https://doi.org/10.1016/j.rse.2020.112204).
- Dorais, L., and Kettela, E.G. (Editors). 1982. A review of entomological survey and assessment techniques used in regional spruce budworm, *Choristoneura fumiferana* (Clem.), surveys and in the assessment of operational spray programs. Report, Committee for Standardization of Survey and Assessment Techniques. Eastern Spruce Budworm Council, Quebec Department of Energy and Resources, Quebec.
- Dormann, C.F., Elith, J., Bacher, S., Buchmann, C., Carl, G., Carré, G., et al. 2013. Collinearity: a review of methods to deal with it and a simulation study evaluating their performance. *Ecography*, **36**: 27–46. doi:[10.1111/j.1600-0587.2012.07348.x](https://doi.org/10.1111/j.1600-0587.2012.07348.x).
- Environment Systems Research Institute (ESRI). 2023. ArcGIS Pro: Version 3.1.3. Redlands, CA.
- Erdle, T.A., and MacLean, D.A. 1999. Stand growth model calibration for use in forest pest impact assessment. *For. Chron.* **75**: 141–152. doi:[10.5558/tfc75141-1](https://doi.org/10.5558/tfc75141-1).
- Fettes, J.J. 1950. Investigations of sampling techniques for population studies of the spruce budworm on balsam fir in Ontario. *Forest Insect Laboratory, Sault Ste. Marie, Ont., Ann. Tech. Rep.* **4**. pp. 163–401.

- Hall, R.J., Castilla, G., White, J.C., Cooke, B.J., and Skakun, R.S. 2016. Remote sensing of forest pest damage: a review and lessons learned from a Canadian perspective. *Can. Entomol.* **148**: S296–S356. doi:10.4039/tce.2016.11.
- Hardy, Y., Mainville, M., and Schmitt, D.M. 1986. An atlas of spruce budworm defoliation in eastern North America 1938–1980. USDA For. Serv., Spruce Budworm Handbook, Misc. Publ. 1449.
- Harrison, X.A., Donaldson, L., Correa-Cano, M.E., Evans, J., Fisher, D.N., Goodwin, C.E.D., et al. 2018. A brief introduction to mixed effects modelling and multi-model inference in ecology. *PeerJ*, **6**: e4794. doi:10.7717/peerj.4794. PMID: 29844961.
- Hennigar, C.R., MacLean, D.A., Quiring, D.T., and Kershaw, J.A. 2008. Differences in spruce budworm defoliation among balsam fir and white, red, and black spruce. *For. Sci.* **54**(2): 158–166.
- Houndode, D.J., Krause, C., and Morin, H. 2021. Predicting balsam fir mortality in boreal stands affected by spruce budworm. *For. Ecol. Manage.* **496**: 119408. doi:10.1016/j.foreco.2021.119408.
- Johns, R.C., Bowden, J.J., Carleton, D.R., Cooke, B.J., Edwards, S., Emilson, E.J.S., et al. 2019. A conceptual framework for the Spruce Budworm Early Intervention Strategy: can outbreaks be stopped? *Forests*, **10**: 910. doi:10.3390/f10100910.
- Kälin, U., Lang, N., Hug, C., Gessler, A., and Wegner, J.D. 2019. Defoliation estimation of forest trees from ground-level images. *Remote Sens. Environ.* **223**: 143–153. doi:10.1016/j.rse.2018.12.021.
- Kettela, E.G. 1983. A cartographic history of spruce budworm defoliation 1967–1981 in eastern North America. Canadian Forestry Service, Maritime Forest Research Centre, Fredericton, NB, Canada. Inf. Rep. DPC-X-14.
- Lenth, R.V. 2023. emmeans: estimated marginal means, aka least-squares means. R package version 1.8.8. Available from <https://cran.r-project.org/package=emmeans> [accessed 15 December 2023]
- Lévesque, R.C., Cusson, M., and Lucarotti, C. 2010. BEGAB: budworm ecogenomics: applications & biotechnology. Institut de biologie intégrative et des systèmes, Université Laval, Québec City, QC.
- Liu, E.Y., Lantz, V.A., MacLean, D.A., and Hennigar, C. 2019. Economics of early intervention to suppress a potential spruce budworm outbreak on crown land in New Brunswick, Canada. *Forests*, **10**(481). PMID: 37180360.
- MacLean, D.A. 1980. Vulnerability of fir–spruce stands during uncontrolled spruce budworm outbreaks: a review and discussion. *For. Chron.* **56**: 213–221. doi:10.5558/tfc56213-5.
- MacLean, D.A., and Lidstone, R.G. 1982. Defoliation by spruce budworm: estimation by ocular and shoot-count methods and variability among branches, trees, and stands. *Can. J. For. Res.* **12**: 582–594. doi:10.1139/x82-090.
- MacLean, D.A., and MacKinnon, W.E. 1996. Accuracy of aerial sketch-mapping estimates of spruce budworm defoliation in New Brunswick. *Can. J. For. Res.* **26**: 2099–2108. doi:10.1139/x26-238.
- MacLean, D.A., and MacKinnon, W.E. 1998. Sample sizes required to estimate defoliation of spruce and balsam fir caused by spruce budworm accurately. *N. J. Appl. For.* **15**: 135–140. doi:10.1093/njaf/15.3.135.
- MacLean, D.A., and Morgan, M.G. 1981. The use of phyllotaxis in estimating defoliation of individual balsam fir shoots. *Can. For. Serv. Res. Notes*, **1**(2): 12–14.
- MacLean, D.A., Erdle, T.A., MacKinnon, W.E., Porter, K.B., Beaton, K.P., Cormier, G., et al. 2001. The Spruce Budworm Decision Support System: forest protection planning to sustain long-term wood supply. *Can. J. For. Res.* **31**: 1742–1757. doi:10.1139/x01-102.
- MacLean, D.A., Amirault, P., Amos-Binks, L., Carleton, D., Hennigar, C., Johns, R., and Régnière, J. 2019. Positive results of an early intervention strategy to suppress a spruce budworm outbreak after five years of trials. *Forests*, **10**: 448. doi:10.3390/f10050448.
- McNie, P., Kneeshaw, D., and Filotas, E. 2023. Landscape-scale patterns of eastern spruce budworm outbreak risk: defoliation onset vs. tree mortality. *Ecosphere*, **14**: e4684. doi:10.1002/ecs2.4684.
- New Brunswick Department of Natural Resources and Energy Development (NBDNRED). 2022. Summary of forest pest conditions 2021. NB Dept. Natural Resources and Energy Devel., Forest Health Section, Fredericton, NB. p. 27.
- New Brunswick Department of Natural Resources and Energy Development (NBDNRED). 2023. Summary of forest pest conditions 2022. NB Dept. Natural Resources and Energy Devel., Forest Health Section, Fredericton, NB. p. 30.
- Ostaff, D.P., and MacLean, D.A. 1995. Patterns of balsam fir foliar production and growth in relation to defoliation by spruce budworm. *Can. J. For. Res.* **25**: 1128–1136. doi:10.1139/x95-125.
- Piène, H., MacLean, D.A., and Wall, R.E. 1981. Effects of spruce budworm-caused defoliation on the growth of balsam fir: experimental design and methodology. Canadian Forest Service, Fredericton, NB, Canada. Inf. Rep. M-X-128.
- Québec Ministère des Forêts de la Faune et des Parcs (QMFFP). 2021. Aires infestées par la tordeuse des bourgeons de l'épinette au Québec en 2021. Québec, gouvernement du Québec, Direction de la protection des forêts. p. 22.
- Québec Ministère des Forêts de la Faune et des Parcs (QMFFP). 2022. Aires infestées par la tordeuse des bourgeons de l'épinette au Québec en 2022. Québec Ministère des Forêts de la Faune et des Parcs, Direction de la protection des forêts, Québec. p. 25.
- Québec Ministère des Ressources Naturelles et des Forêts (QMRNF). 2023. Aires infestées par la tordeuse des bourgeons de l'épinette au Québec en 2023. Québec Ministère des Ressources Naturelles et des Forêts, Direction de la protection des forêts, Québec. p. 34.
- Quinn, G.P., and Keough, M.J. 2002. Experimental design and data analysis for biologists. Cambridge University Press, Cambridge, UK.
- R Core Team. 2023. R: a language and environment for statistical computing. R Foundation for Statistical Computing, Vienna, Austria. Available from <https://www.R-project.org/> [accessed 15 December 2023]
- Rahimzadeh-Bajgiran, P., Weiskittel, A., Kneeshaw, D., and MacLean, D. 2018. Detection of annual spruce budworm defoliation and severity classification using Landsat imagery. *Forests*, **9**: 357. doi:10.3390/f9060357.
- Rowe, J.S. 1972. Forest regions of Canada. Canadian Forestry Service. Ottawa, Canada. Publication 1300.
- Sanders, C.J., (Compiler). 1980. A summary of current techniques used for sampling spruce budworm populations and estimating defoliation in eastern Canada. *Can. For. Serv. Inf. Rep.* O-X-306.
- Sidhu, H.K., Kidd, K.A., Emilson, E.J.S., Stastny, M., Venier, L., Kielstra, B.W., and McCarter, C.P.R. 2024. Increasing spruce budworm defoliation increases catchment discharge in conifer forests. *Sci. Total Environ.* **912**: 168561. doi:10.1016/j.scitotenv.2023.168561.
- Stehman, S.V., and Foody, G.M. 2019. Key issues in rigorous accuracy assessment of land cover products. *Remote Sens. Environ.* **231**: 111199. doi:10.1016/j.rse.2019.05.018.
- Taylor, S.L., and MacLean, D.A. 2008. Validation of spruce budworm outbreak history developed from aerial sketch mapping of defoliation in New Brunswick. *N. J. Appl. For.* **25**(3): 139–145. doi:10.1093/njaf/25.3.139.
- Waters, W.E., Heller, R.C., and Bean, J.L. 1958. Aerial appraisal of damage by spruce budworm. *J. For.* **56**: 269–276.
- Wickham, H. 2016. ggplot2: elegant graphics for data analysis. Springer-Verlag New York. Available from <http://ggplot2.tidyverse.org> [accessed 15 December 2023]
- Woodman, S.G., Khoury, S., Fournier, R.E., Emilson, E.J.S., Gunn, J.M., Rusak, J.A., and Tanentzap, A.J. 2021. Forest defoliator outbreaks alter nutrient cycling in northern waters. *Nat. Commun.* **12**: 6355. doi:10.1038/s41467-021-26666-1.
- Zuur, A.F., Ieno, E.N., Walker, N.J., Saveliev, A.A., and Smith, G.M. 2009. Mixed effects models and extensions in ecology with R. Springer.